

Use of computer modeling for defect engineering in Czochralski silicon growth

V. Artemyev^{a,*}, A. Smirnov^{a,b}, V. Kalaev^{a,b}, V. Mamedov^b, A. Sid'ko^b, T. Wejrzanowski^c, M. Grybczuk^c, P. Dold^d, R. Kunert^d

^aSTR Group, Inc., 64 Bolshoi Sampsonievskii pr., Build. "E", Office 605, St. Petersburg, 194044, Russian Federation

^bSoft-Impact, Ltd., 64 Bolshoi Sampsonievskii pr., Build. "E", Office 603, St. Petersburg, 194044, Russian Federation

^cWarsaw University of Technology, Faculty of Materials Science and Engineering, Woloska 141, 02-507 Warsaw, Poland

^dFraunhofer Center for Silicon Photovoltaics CSP, Otto-Eissfeldt-Strasse 12, 06120 Halle, Germany

Abstract

The yield and quality of silicon wafers are mostly determined by defects, including grain boundaries, dislocations, vacancies, interstitials, and vacancy and oxygen clusters. Active generation and multiplication of dislocations during Czochralski mono-silicon crystal growth is almost always followed by a transition to multicrystalline material and is called structure loss. Possible factors in structure loss are related to high thermal stresses, fluctuations of local crystallization rate caused by melt flow turbulence, melt undercooling and incorporation of solid particles from the melt into the crystal. Experimental analysis of dislocation density distributions in grown crystals contributes to an understanding of the key reasons for structure loss: particle incorporation at the crystallization front and strong fluctuations of crystallization rate with temporal remelting. Comparison of experimental dislocation density measurements and modeling results calculated using the Alexander-Haasen model showed good agreement for silicon samples. The Alexander-Haasen model provides reasonably accurate results for dislocation density accompanying structure loss phenomena and can be used to predict dislocation density and residual stresses in multicrystalline Czochralski silicon ingots, which are grown for the purpose of manufacturing polysilicon rods for Siemens reactors and silicon construction elements.

Keywords: Czochralski silicon growth, structure loss, dislocation density

1. Introduction

There is a drive to increase silicon crystal yield to meet the challenges of the photovoltaics market [1] and in the production of electronics. The main issue for Czochralski (Cz) mono-silicon crystal growth is improving crystal quality through controlling the concentration and clusterization of self point defects [2], the level of impurities [3], twisting [4] and structure loss [5–7]. In this paper, we discuss possible reasons for monocrystalline structure loss with subsequent generation, multiplication and propagation of dislocations in the bulk crystal, and perform analysis of how these factors contribute to the structure loss observed in the actual Cz silicon growth process. Analysis of the reasons for structure loss is very important from the angle of retaining the monocrystalline structure in Cz silicon both for photovoltaics and electronic applications, because yield falls significantly if structure loss necessitates further remelting of the crystal part with dislocations [8]. In the literature [5–7, 9], possible reasons for structure loss and improvement solutions are

discussed, but there is still no common opinion on the main reason for structure loss.

An experimental approach to solving these problems requires multiple crystal growth experiments together with characterization procedures. Combining computer modeling with experimental work significantly helps accelerate—and cut the cost of—process development and optimization.

Structure loss was observed during research growth of 4-inch and 8-inch silicon crystals in the facility of Fraunhofer CSP. Experimental data contains maps with dislocation density distribution in silicon samples cut at different crystal heights. From analysis of such distributions, we suggested the major reason for structure loss for each crystal. Unsteady computer modeling using CGSim software was performed to calculate the dislocation density in two crystals using the Alexander-Haasen model [10]. The calculated results were then compared to experimental data.

2. Experimental approach

Samples of monocrystalline Czochralski 4-inch and 8-inch silicon crystals were cut in such a way that they represented the material both before and after structure loss. Further

*Corresponding author

Email address: vladimir.artemyev@str-soft.com (V. Artemyev)

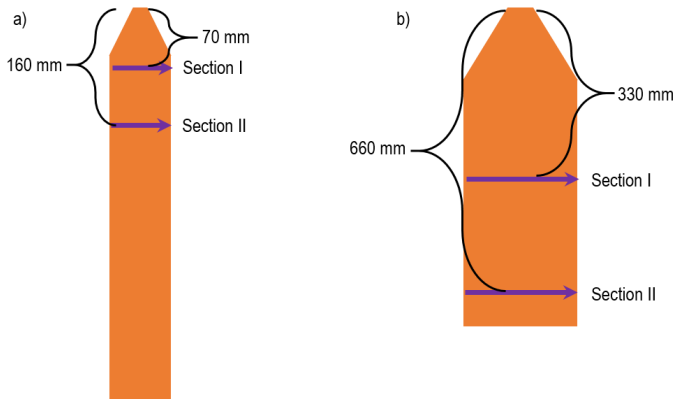


Figure 1: Schematic of crystal cutting: a) 4-inch ; b) 8-inch

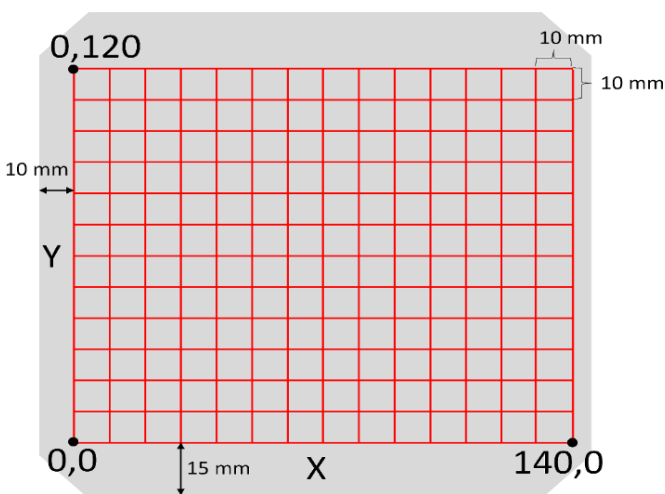


Figure 2: Schematic of sample surface mapping

macro and microscopic observations were performed for selected samples. In Fig.1 the scheme of crystals is illustrated: section I corresponds to the samples before structure loss, section II corresponds to the samples after structure loss.

Observations of the samples were performed using NIKON LV150 microscope equipped with a motorized sample position system. Images were taken for the purpose of creating an etch pit density (EPD) map of the sample surface. 195 pictures were taken for each sample, creating a 15x13 image matrix, with the distance between matrix points equal to 1 cm on both the x and y axis, as presented in Fig. 2. The directions of the axes were chosen arbitrarily for each sample.

Image analysis was performed using Semiconductor Defect Analyzer (SDA) software [11, 12], which was used to improve picture quality and perform binarization and counting of distinct elements in the picture. Using the application every image series was automatically analyzed using the same settings. The image transformations were chosen to extract etch pits and minimize the counting of artefacts such as dust and scratches. An example of image processing effects is shown in Fig. 3. Every black element remaining after image

processing was counted by the SDA as a defect for mapping purposes.

Since etching and analysis of etched images is difficult, it is important to discover and recognize meaningful elements of the structures. Objects which appeared on samples after etching and which were subsequently counted, are circled in red in Fig. 4.

For every image group slightly elongated, uniformly black objects were counted, since they were identified as Secco etch pits [13]. Areas covered with black circular dots which had bright centers were observed in every image group. The size of the dots varied, but they were generally smaller than Secco etch pits. As their origin remained unidentified at the time of analysis, they were not taken into account. Image processing steps (mainly thresholding and erosion) were parametrized in a way that eliminated most of the small dots before the defects were counted by the software. A few examples of round dots of unknown origin (uncounted) were marked with yellow circles.

3. Numerical model

CGSim software [14] was used to simulate Czochralski unsteady silicon crystal growth in 2D axisymmetric approximation. The governing equations, boundary conditions and method approach are considered in [9, 14]. Computer simulation includes: heat conduction in the entire computational domain, melt convection, radiation by surface-to-surface method, crystal/melt interface evolution, calculation of the meniscus shape near the crystal/melt triple point and melt/crucible point. A schematic chart of the furnace for silicon crystal growth is presented in Fig. 5. At the first stage of unsteady modeling, experimental verification of the silicon crystal growth model was performed by analysis of global heat transfer. Calculated and experimental results of the absolute value of heater power were compared. In Fig. 6 heater power evolution is presented for 4-inch. The difference between the model and experiment is less than 2%. Besides predicting heater power, it is also very important to predict the spatial distribution of heat flux inside the furnace. This distribution can be analyzed by calculating heat losses in water cooling systems, using inlet and outlet water temperature and the water flow rate. The comparison presented in table 1 gives us average absolute values and ratios of heat losses in different water cooling systems for 4-inch silicon growth process with 3% discrepancy in the ratio between holder and chamber parts systems, which can be explained due to an error in inlet water temperature measurements during crystal pulling. The crystal growth model quite reasonably reproduces heater power evolution and heat flux spatial distribution in the furnace, defining correct temperature gradient distribution in the whole system, so it can be successfully used for further analysis and prediction of dislocation density.

At the second stage, the multiplication of dislocations was analyzed using the Alexander-Haasen model with parameters presented in table 2. All parameters defined in [15], except the Peierls potential and material constant p , which

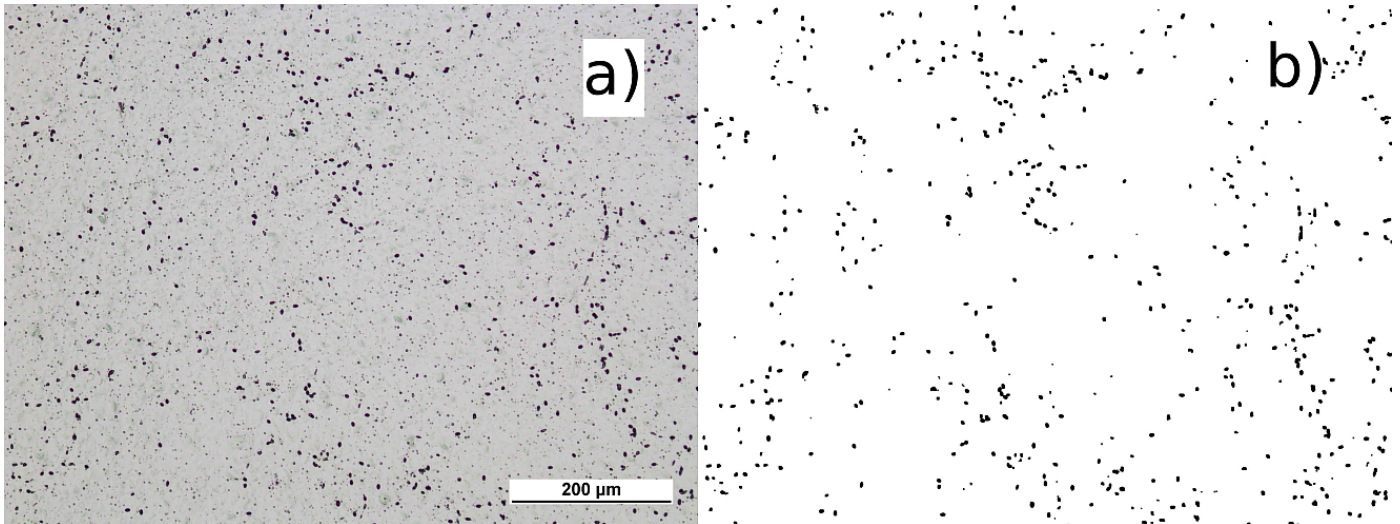


Figure 3: Example of image processing effects: a) original photo; b) processed picture

Table 1: Heat losses in the water cooling systems

	Experiment, kW	Experiment ratio	CGSim, kW	CGSim ratio
Holder cooling system	5.46	13%	5.16	10%
Chamber parts cooling system	37.46	86%	44.43	89%
Crucible shaft cooling system	0.45	1%	0.51	1%

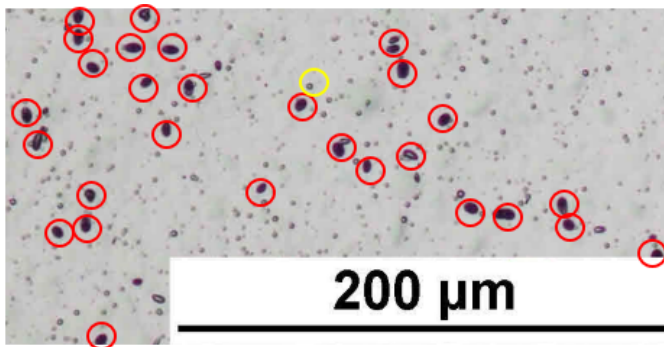


Figure 4: Objects counted on image

Table 2: Parameters of Alexander-Haasen model for silicon

Parameter	Value
Burger's vector b , m	$3.8e-10$
Relative strain hardening factor R	0.8165
Material constant p	as temperature function [16]
Material constant l	1
Material constant k_0 , $m^{2p+1}/NP/s$	$8.58e-4$
Material constant K , m/N	$3.10e-4$
Peierls potential Q , eV	as stress function [16]
Young's modulus E , Pa	$1.653e11$
Poisson's ratio ν	0.217

were obtained as a function of stresses and temperature respectively in [16]. The model description and dislocation density transfer approach at the crystal/melt interface was described in [17]. The computer simulation with relaxation of thermal stress into the dislocation density was performed from the point of structure loss through to the end of the growth stage for both crystals: from 160 mm of crystal length for 4-inch and from 425 mm of crystal length for 8-inch crystal.

4. Results and discussion

Structure loss in the crystal growth process is accompanied by the disappearance of one or several growth nodes on the side surface of the crystal, with rapid generation of

dislocations at the point of structure loss and its further penetration and multiplication during crystal pulling. The uncertainty as to the exact spatial location of the origin of structure loss adds an extra layer of complexity to fixing the problem. Hence, it is important to find the factors affecting the generation of dislocations.

Let us consider possible reasons for structure loss at a point inside the crystal: high thermal stress in the crystal [5, 6], strong fluctuations of the crystallization rate at the crystal/melt interface shape due to turbulent melt convection [5], particle incorporation at the crystallization front [6, 7], mechanical vibration of the crystal and waves on the melt

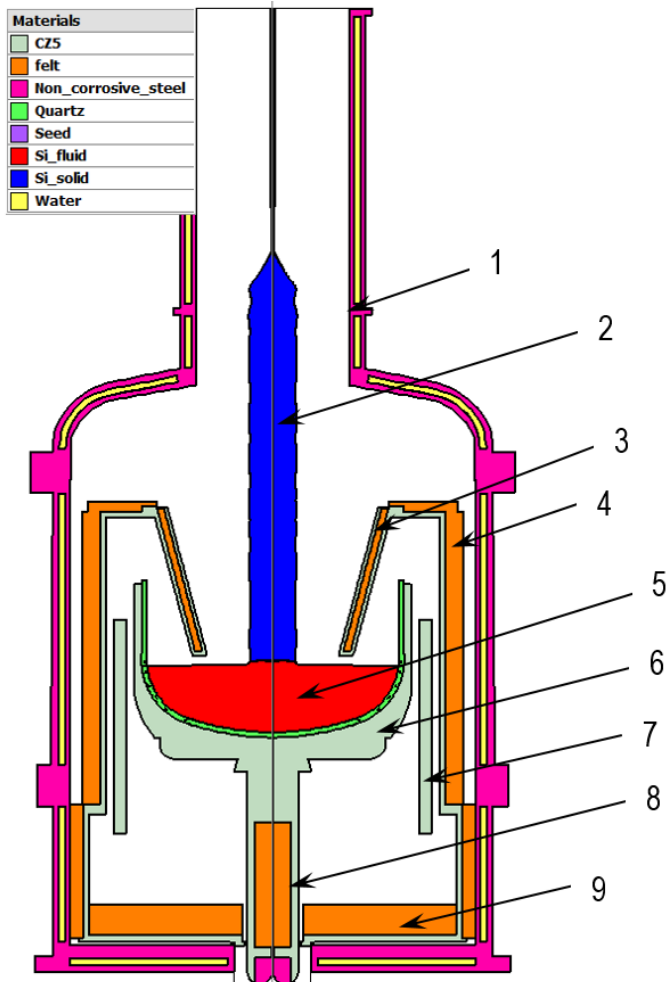


Figure 5: Schematic chart of furnace: 1) steel shield; 2) silicon crystal; 3) heat shield; 4) side insulation; 5) silicon melt; 6) graphite crucible; 7) heater; 8) pedestal; 9) bottom insulation

free surface [5].

The thermal elastic shear stress distributions are presented in Fig. 7 for both crystals for the growth stage before the structure loss. The absolute values and distributions of the shear stress are defined by the crystal temperature and mechanical properties of silicon.

In the paper [18], generation of dislocations is expected when shear stresses exceed the critical resolved shear stress (CRSS). The CRSS value is an ascending function of temperature [18]; for $T=1685$ K the CRSS value is 1.57 MPa using extrapolation of the data in [18]. From the distribution in Fig. 7 the global maximum shear stress is about 12 MPa at the periphery of the crystal, 7 MPa and 10 MPa for 4-inch and 8-inch boules respectively at the melt/crystal interface, but no dislocations are observed. It is well known that growth of dislocation-free silicon crystals may take place with higher shear stress than CRSS: in our crystals, the typical value of stress is about 10 MPa for the moment before structure loss. We suggest that shear stress is not a sufficient reason for the onset of structure loss with generation of dislocation density, but high shear stress promotes the mul-

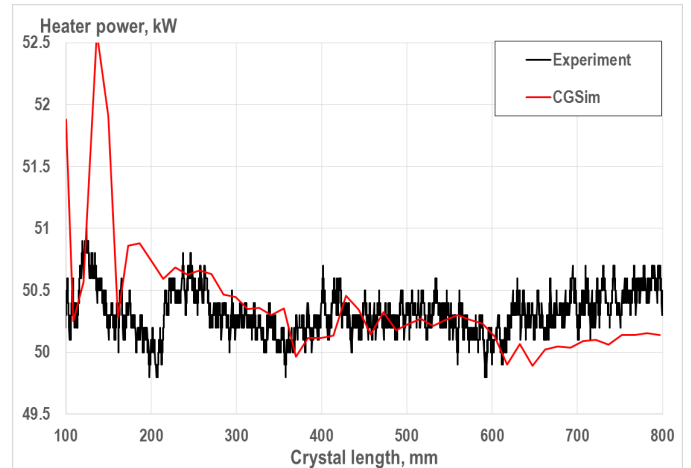


Figure 6: The heater power evolution

tiplication of dislocations through the relaxation of stress into the dislocation density.

High fluctuations of the crystallization rate at the melt/crystal interface with temporal crystal remelting may be the principal reason for structure loss, due to disturbance of the crystal lattice accompanied by a lattice misfit. To investigate this reason, 3D unsteady computer modeling should be conducted as in [4, 5], which requires significant time and computer resources. We performed 3D computer modeling for the 8-inch crystal growth process and observed temporal small negative fluctuations of the crystallization rate with typical value of -0.2 mm/min at the melt/crystal interface. Such remelting can result in instability of the crystallization interface and may increase the probability of dislocation generation.

We suppose that fluctuations in the crystallization rate together with high shear stress are the major reasons for structure loss for 8-inch crystal. Suppression of the crystallization rate fluctuations could provide a solution to the problem: the same approach with additional optimization of furnace design and process parameters is discussed in the paper [5].

For 4-inch ingot, one factor reduces the probability of local crystal remelting at the melt/crystal interface: for the higher crystal pulling rate, much stronger temperature fluctuations in the melt are required to obtain negative crystallization rates at the melt/crystal interface.

The formation of solid particles may take place as a result of chemical reactions in the gas and along the solid walls above the melt free surface [3]. After deposition, these particles may fall down into the melt and be incorporated into the crystal. Incorporation of a solid particle into the crystal will most likely cause structure loss due to either misorientation between the particle and silicon crystal, or local concentration of thermal stress due to different thermal expansion coefficients of the silicon crystal and parasitic particle. We suspect that a phenomenon of this sort was responsible for structure loss with transition from dislocation-free growth to growth with dislocations near the melt/crystal interface for the

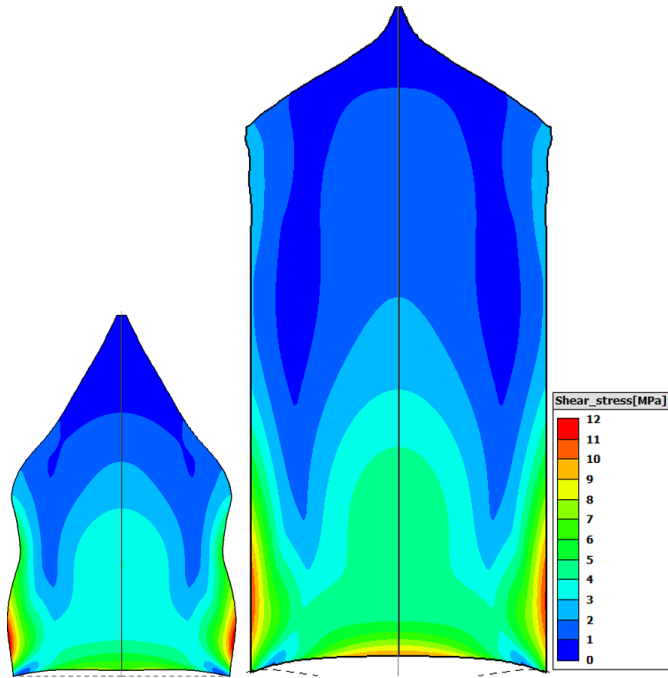


Figure 7: Thermal elastic shear stress distribution before structure loss for 4-inch (left) and 8-inch (right) crystals

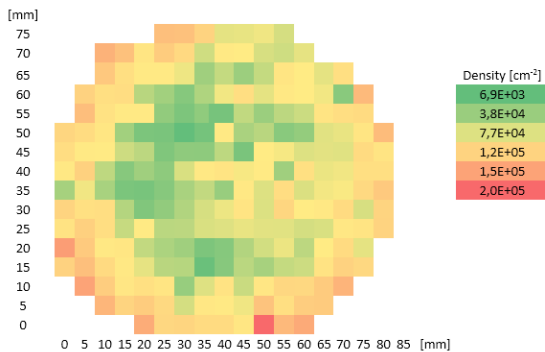


Figure 8: Experimental radial dislocation density distribution (4-inch) for section I

4-inch crystal under consideration.

Let us discuss the experimental data and results of computer simulation of dislocation density for 4-inch crystal with [100] pulling direction. Radial distribution of experimental dislocation density in Fig. 8 shows deep penetration of dislocations in the upper part of the crystal sample (section I) up to the seed with average dislocation density value of $1 \cdot 10^5 \text{ cm}^{-2}$. Higher density of etch pits is observed at the crystal periphery, with a typical value of $6 \cdot 10^5 \text{ cm}^{-2}$ for section II, Fig. 9. From vertical distribution in Fig. 10, the dislocations slide along [111] direction and radial dislocation density distribution becomes more uniform towards the bottom part of the crystal. Similar propagation of dislocations is considered in paper [6], where the authors suggested that particle incorporation at the periphery of the crystal is a possible reason for structure loss with subsequent generation of dislocations.

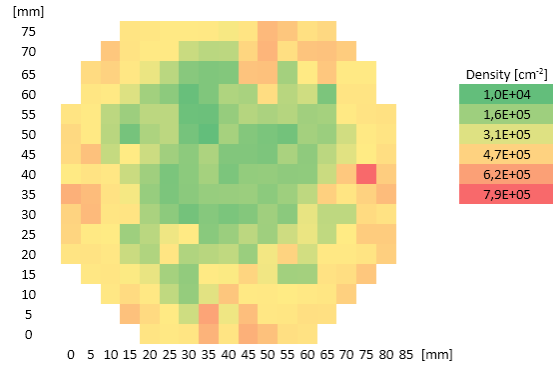


Figure 9: Experimental radial dislocation density distribution (4-inch) for section II

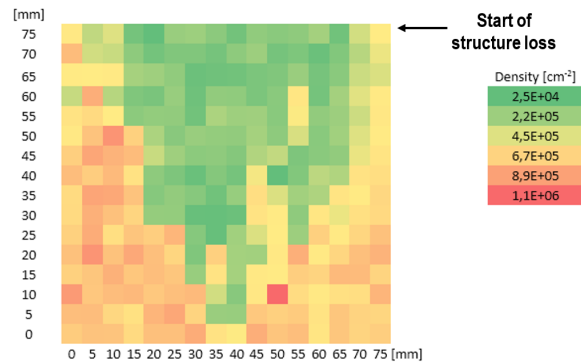


Figure 10: Experimental vertical dislocation density distribution (4-inch)

Unsteady simulation of dislocation density multiplication in the Alexander-Haasen model requires definition of initial dislocation density in the crystal. For all calculations, a low initial dislocation density value of $N_0=10 \text{ cm}^{-2}$ was used. We compared the calculated and experimental radial distribution for section II (Fig. 9) and found good agreement only for the central crystal part, as illustrated in Fig. 11, and a significant discrepancy at the crystal periphery. This difference could be explained by the high initial dislocation density at the crystal periphery, generated after incorporation of a solid particle. However, from the experiment, it is difficult to estimate the local dislocation density generated in the peripheral area.

From experimental measurements of dislocation density distribution for 8-inch only, individual etch pits are observed in section I, located above the point of monocrystalline structure loss (Fig. 12). The total number of dislocations ranged from 3 to 10 for the whole horizontal cross-section. High dislocation density at the crystal centre of $2 \cdot 10^5 \text{ cm}^{-2}$ and occasional areas of high dislocation density near the edges were observed for section II, located below the point of structure loss (Fig. 13). Radial distributions of the dislocation density for calculated and experiment results are illustrated in Fig. 14 for section II. Good agreement is found between the experimental and calculated results with 20% deviation. The Alexander-Haasen model provided more accurate results for 8-inch crystal, where evolution of dislocations was more governed by thermal stress. It is also worth noting that while

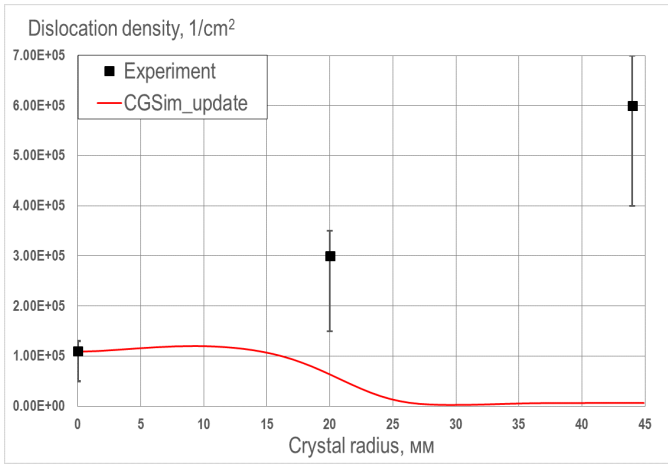


Figure 11: Dislocation density comparison for section II, 4-inch

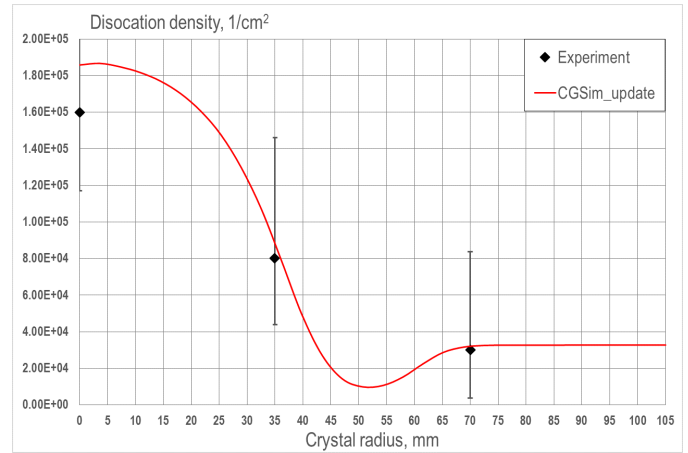


Figure 14: Dislocation density comparison for section II, 8-inch

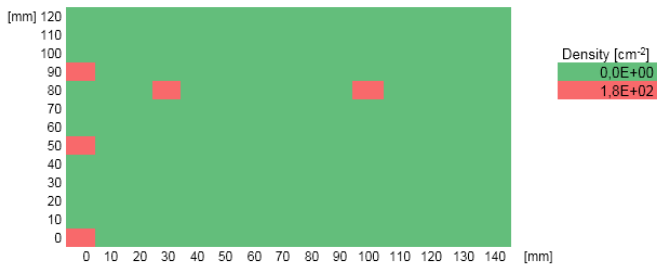


Figure 12: Experimental dislocation density distribution (8-inch) for section I

both crystals have similar EPD in the center with higher values for 8-inch crystal, the EPD at the periphery of 4-inch crystal is more than one order of magnitude higher than EPD at the periphery of 8-inch crystal, while thermal stress was lower. This indicates that the high EPD at the periphery of 4-inch crystal is most likely caused by an external force, such as incorporation of an impurity solid particle.

5. Conclusion

Structure loss was analyzed during Czochralski monocrystalline silicon growth for crystals with 4-inch and 8-inch diameters. Much higher dislocation density for 4-inch crystal at the crystal periphery compared to 8-inch crystal probably indicated a different origin of monocrystalline structure loss.

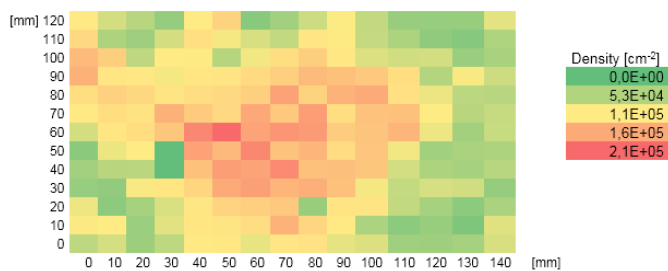


Figure 13: Experimental dislocation density distribution (8-inch) for section II

Verification of a 2D axisymmetric computer model of 4-inch and 8-inch Czochralski silicon crystal growth was done using global heat transfer parameters: power heater and heat loss distribution. The Alexander-Haasen model was used to produce calculations for the dislocation multiplication process.

Based on experimental and modeling results, we suggested major reasons for structure loss for both crystals: fluctuations of the crystallization rate with high shear stress at the crystal/melt interface shape for 8-inch crystal; incorporation of impurity solid particles at the crystallization front for 4-inch crystal.

Comprehensive computer simulation of dislocation density multiplication within the Alexander-Haasen model quite reasonably predicted dislocation density in the center for both crystals and radial distribution for 8-inch crystal. It was difficult to predict the radial dislocation density distribution for 4-inch crystal due to uncertainty because of the local stress generation by incorporating solid particle.

The Alexander-Haasen model can be useful for analyzing the structure loss phenomenon and for predicting dislocation density and residual stresses in multicrystalline Czochralski silicon ingots grown for the production of rods for Siemens reactors.

Acknowledgements

This work was supported by the Foundation for Assistance to Small Innovative Enterprises (FASIE, Russia) within the framework of international program ERA.Net RUS Plus [project ERA-RUS-15109]. The study was also financially supported by the Polish National Center for Research and Development under contract No 1/RUSPLUS-INNO/2015.

References

[1] Fraunhofer ise: Photovoltaics report, available online: www.ise.fraunhofer.de/content/dam/ise/de/documents/publications/studies/photovoltaics-report.pdf (2018).

- [2] M. S. Kulkarni, J. C. Holzer, L. W. Ferry, The agglomeration dynamics of self-interstitials in growing czochralski silicon crystals, *Journal of Crystal Growth* 284 (3) (2005) 353 – 368. doi:10.1016/j.jcrysgro.2005.07.041.
- [3] A. Vorob'ev, A. Sid'ko, V. Kalaev, Advanced chemical model for analysis of cz and ds si-crystal growth, *Journal of Crystal Growth* 386 (2014) 226 – 234. doi:10.1016/j.jcrysgro.2013.10.022.
- [4] V. Kalaev, A. Sattler, L. Kadinski, Crystal twisting in cz si growth, *Journal of Crystal Growth* 413 (2015) 12 – 16. doi:10.1016/j.jcrysgro.2014.12.005.
- [5] O. Smirnova, N. Durnev, K. Shandrakova, E. Mizitov, V. Soklakov, Optimization of furnace design and growth parameters for si cz growth, using numerical simulation, *Journal of Crystal Growth* 310 (7) (2008) 2185 – 2191, the Proceedings of the 15th International Conference on Crystal Growth (ICCG-15) in conjunction with the International Conference on Vapor Growth and Epitaxy and the US Biennial Workshop on Organometallic Vapor Phase Epitaxy. doi:10.1016/j.jcrysgro.2007.11.204.
- [6] A. Lanterne, G. Gaspar, Y. Hu, E. Øvrelid, M. D. Sabatino, Investigation of different cases of dislocation generation during industrial cz silicon pulling, *physica status solidi (c)* 13 (10-12) (2016) 827–832. doi:10.1002/pssc.201600063.
- [7] A. Lanterne, G. Gaspar, Y. Hu, E. Øvrelid, M. D. Sabatino, Characterization of the loss of the dislocation-free growth during czochralski silicon pulling, *Journal of Crystal Growth* 458 (2017) 120 – 128. doi:10.1016/j.jcrysgro.2016.10.077.
- [8] Y. Wang, K. Kakimoto, An in-situ x-ray topography observation of dislocations, crystal-melt interface and melting of silicon, *Microelectronic Engineering* 56 (1) (2001) 143 – 146, sub-Quarter-Micron Silicon Issues in the 200/300 mm Conversion Era. doi:10.1016/S0167-9317(00)00517-7.
- [9] A. Giannattasio, S. Senkader, R. J. Falster, P. R. Wilshaw, Generation of dislocation glide loops in czochralski silicon, *Journal of Physics: Condensed Matter* 14 (48) (2002) 12981.
- [10] H. Alexander, P. Haasen, Dislocations and plastic flow in the diamond structure, Vol. 22 of *Solid State Physics*, Academic Press, 1969, pp. 27 – 158. doi:10.1016/S0081-1947(08)60031-4.
- [11] T. Wejrzanowski, K. J. Kurzydowski, Stereology of grains in nano-crystals, *Solid State Phenomena* 94 (2003) 221–228. doi:10.4028/www.scientific.net/SSP.94.221.
- [12] T. Wejrzanowski, W. Spychalski, K. Rozniatowski, K. Kurzydowski, Image based analysis of complex microstructures of engineering materials, *International Journal of Applied Mathematics and Computer Science* 18 (1) (2008) 33–39. doi:10.2478/v10006-008-0003-1.
- [13] F. Secco d' Aragona, Dislocation etch for (100) planes in silicon, *Journal of The Electrochemical Society* 119 (7) (1972) 948–951. doi:10.1149/1.2404374.
- [14] CGSim Flow Module, Theory Manual, Version 16.1, STR IP Holding, Richmond, VA, USA, 2017.
- [15] B. Gao, S. Nakano, K. Kakimoto, Highly efficient and stable implementation of the alexander-haasen model for numerical analysis of dislocation in crystal growth, *Journal of Crystal Growth* 369 (2013) 32 – 37. doi:10.1016/j.jcrysgro.2013.01.039.
- [16] V. N. Erofeev, V. I. Nikitenko, Comparison of theory of dislocation mobility with experimental data for silicon, *Soviet Physics Jetp* 33 (5).
- [17] V. Artemyev, A. Smirnov, V. Kalaev, V. Mamedov, A. Sidko, O. Podkopaev, E. Kravtsova, A. Shimansky, Modeling of dislocation dynamics in germanium czochralski growth, *Journal of Crystal Growth* 468 (2017) 443 – 447, the 18th International Conference on Crystal Growth and Epitaxy (ICCGE-18). doi:10.1016/j.jcrysgro.2017.01.032.
- [18] N. Miyazaki, H. Uchida, T. Munakata, K. Fujioka, Y. Sugino, Thermal stress analysis of silicon bulk single crystal during czochralski growth, *Journal of Crystal Growth* 125 (1) (1992) 102 – 111. doi:10.1016/0022-0248(92)90325-D.